Nuclear Engineering and Technology 53 (2021) 439–445

Contents lists available at ScienceDirect

Nuclear Engineering and Technology

journal homepage: www.elsevier.com/locate/net

Original Article

Applicability research of round tube CHF mechanistic model in rod bundle channel

Wei Liu [a, *], Shinian Peng [a], Jianqiang Shan [b], Guangming Jiang [a], Yu Liu [a], Jian Deng [a], Ying Hu [a]

[a] Nuclear Power Institute of China, State Key Laboratory of Reactor System Design Technology, Chengdu, 610213, China
[b] Xi'an Jiaotong University, School of Nuclear Science and Technology, Xi'an, 710049, China

ARTICLE INFO

Article history:
Received 5 May 2020
Received in revised form
23 June 2020
Accepted 15 July 2020
Available online 29 July 2020

Keywords:
Round tube
Critical heat flux
Mechanistic model
Rod bundle channel

ABSTRACT

In view of the complex geometric structure of the rod bundle channel and the limitation of the current CHF visualization experiment technology, it is very difficult to obtain the rod bundle CHF mechanism directly through the phenomenon of the rod bundle CHF visualization experiment. In order to obtain the applicable CHF mechanism assumption for rod bundle channel, firstly, five most representative DNB type round tube CHF mechanistic models are obtained with evaluation and screening. Then these original round tube CHF mechanistic models based on inlet conditions are converted to local conditions and coupled with subchannel analysis code ATHAS. Based on 5 × 5 full-length rod bundle CHF experimental data independently developed by Nuclear Power Institute of China (NPIC), the applicability research of each model for CHF prediction performance in rod bundle channel is carried out, and the commonness and difference of each model are comparatively studied. The CHF mechanism assumption of superheated liquid layer depletion that is most likely to be applicable for the rod bundle channel is selected and two directions that need to be improved are given. This study provides a reference for the development of CHF mechanistic model in rod bundle channel.

1. Introduction

The development of critical heat flux (CHF) mechanistic model for flow boiling in round tube started in the 1960s, and the 1970s–1980s were the prime time for its development. So far, it is preliminarily estimated that more than 50 CHF mechanistic models based on various assumptions and constitutive correlations have been developed [1]. These CHF mechanistic models can be divided into three types: (1) homogeneous nucleation type [2], (2) departure from nucleate boiling (DNB) type and (3) dry-out (DO) type [3].

The homogeneous nucleation CHF usually occurs before the onset of significant voiding (OSV) point, which is not the object of this study. Compared with DNB type CHF mechanistic model, researchers have basically mastered the occurrence mechanism of DO type CHF corresponding to high quality and annular flow conditions, and developed some effective models [4–8].

As corresponding to a variety of flow patterns and heat transfer characteristics, the mechanism of DNB type CHF is the most complicated and concerned by researchers. At present, the DNB type CHF mechanism assumptions can be divided into the following categories [9]: (1) liquid layer superheat limit model; (2) boundary layer separation model; (3) liquid flow blockage model; (4) near wall bubble crowding model; (5) liquid sublayer dryout model; (6) interfacial lift-off model; (7) superheated liquid layer depletion model [10] et al.

The existing research results and practical experience show that among the above-mentioned CHF mechanism assumptions, the most widely accepted, developing and representative ones are bubble crowding model proposed by Weisman and Pei [11], liquid sublayer dryout model proposed by Lee and Mudawar [12], and superheated liquid layer depletion model proposed by Chun et al. [10].

In view of the complex geometric structure of the rod bundle channel and the limitation of the current CHF visualization experiment technology, it is very difficult to obtain the rod bundle CHF mechanism directly through the phenomenon of the rod bundle CHF visualization experiment. When developing the rod bundle CHF mechanistic model, a feasible method is to study the

* Corresponding author.
E-mail address: liuwei0958@126.com (W. Liu).

https://doi.org/10.1016/j.net.2020.07.023

applicability of the existing round tube CHF mechanistic model in rod bundle channel, so as to obtain the mechanism assumption most likely to be used in the development of rod bundle CHF mechanistic model.

In this study, the five representative DNB type round tube CHF mechanistic models are screened out. With the heat balance method (HBM) and the direct substitution method (DSM), these original round tube CHF mechanistic models based on inlet conditions are converted to local conditions and coupled with subchannel analysis code ATHAS [11–13]. The applicability research of each model for CHF prediction performance in rod bundle channel is carried out based on 5 × 5 full-length rod bundle CHF experimental data independently developed by NPIC. Then the most robust and applicable CHF mechanism for rod bundle channel is obtained.

2. Selected CHF mechanistic model

In this paper, the principle of selecting CHF mechanistic model applicable for pressurized water reactor (PWR) core is as follows:

(1) Detailed mechanism assumption and derivation process;
(2) Empirical parameters should be minimal;
(3) The application range of the model should apply to PWR operation and accident conditions;
(4) It has been verified with the CHF experimental data by the developers.

Based on the above principles, five most representative DNB type round tube CHF mechanistic models are selected and obtained, and the parameter ranges are shown in Table 1.

The detailed mechanism assumption, derivation process and conservation equation of each CHF model can be found in corresponding references.

3. Calculation method and CHF experimental data

3.1. Calculation method

The CHF phenomenon in PWR rod bundle channel is divided into three modeling scales by Bestion et al. [18], as shown in Fig. 1. Cheng & Müller [19] pointed out that the prediction accuracy of CHF in rod bundle channel depends on the accurate calculation of local two-phase flow parameters, while at present, the computational tools for calculating local two-phase flow parameters include subchannel analysis code and CFD tool.

The computational tool in this paper is subchannel analysis code ATHAS. A detailed description of ATHAS modeling assumptions are presented in Table 2.

On the one hand, the round tube CHF mechanistic models selected in section 2 are all based on the inlet conditions in their initial assumptions, on the other hand, the local parameters in subchannel analysis code ATHAS are based on the local conditions, so it is necessary to convert the CHF mechanistic model under the inlet conditions into the local conditions. There are two methods involved here: the heat balance method (HBM) and the direct substitution method (DSM).

As for the HBM method, when the CHF mechanistic model is used for calculating, firstly, an initial heat flux is assumed and the CHF value of each control volume in the subchannel is predicted. Then, the convergence of the assumed value and the predicted value is judged. If it is not convergent, then the assumed value is increased or decreased until it is convergent. This needs to be calculated iteratively and the variable usually obtained is the critical power.

As for the DSM method, the CHF mechanistic model is similar to the CHF empirical correlation, and both of them can calculate the CHF value based on the local parameters. At this time, there is no need to calculate iteratively and the commonly obtained variable is the local critical heat flux.

In fact, the HBM method is mainly used to calculate the thermal margin in closed fuel assemblies such as BWR and CANDU assemblies, and the DSM method is mainly used for thermal hydraulic design and safety analysis of PWR fuel assemblies after coupling with the subchannel analysis code.

3.2. CHF experimental data

In this paper, the 5 × 5 full-length rod bundle CHF experimental data independently developed by NPIC is used for assessment. The CHF experiments are performed in 5 × 5 rod bundles under various test configurations considering factors such as the rod bundle geometry, the rod radial peaking factors, the rod axial flux shape, and the axial locations and form losses of spacer grids [21]. In total five different CHF test series are selected, as shown in Table 3.

4. Study on the applicability in rod bundle channel

4.1. Result analysis of five CHF models

Without any modification to the original round tube CHF mechanistic model, the CHF prediction accuracy of above models in rod bundle channel are evaluated by using the CHF experimental test 1 in Table 3. The evaluation results are shown in Table 4.

It can be seen that: (1) with the HBM method, compared with the measured CHF value (M), the predicted CHF value (P) of Weisman & Pei model, and Lee & Mudawar and Katto model is about 13% and 25% larger than 1, respectively, while the predicted value of Lin et al. and KAIST model is about 12% smaller than 1; (2) and with the DSM method, the predicted values of Weisman & Pei,

Table 1
Parameter ranges of each CHF model.

Model	The bubble crowding model	The liquid sublayer dryout model			The superheated liquid layer depletion model
	Weisman & Pei [14]	Lee & Mudawar [15]	Lin et al. [16]	Katto [17]	KAIST [10]
Fluid	–	Water	Water	–	–
ρ_v/ρ_l	0.012–0.41	0.032–0.23	0.032–0.23	0.0000051–0.35	0.021–0.245
p(MPa)[a]	2–21	5–17	5–17	0.1–20	3.4–18
G(kg/m^{2}s)	500–13600	1000–5000	1000–5000	–	706–7500
D(mm)	1.15–37.5	4–16	4–16	–	3.6–37.5
L(m)	0.004–3.6	–	–	–	0.08–6
x_l	–	–	–	<0	–
α	<0.8	<0.5	<0.7	<0.7	<0.65

[a] Equivalent pressure in water at equal density ratio.

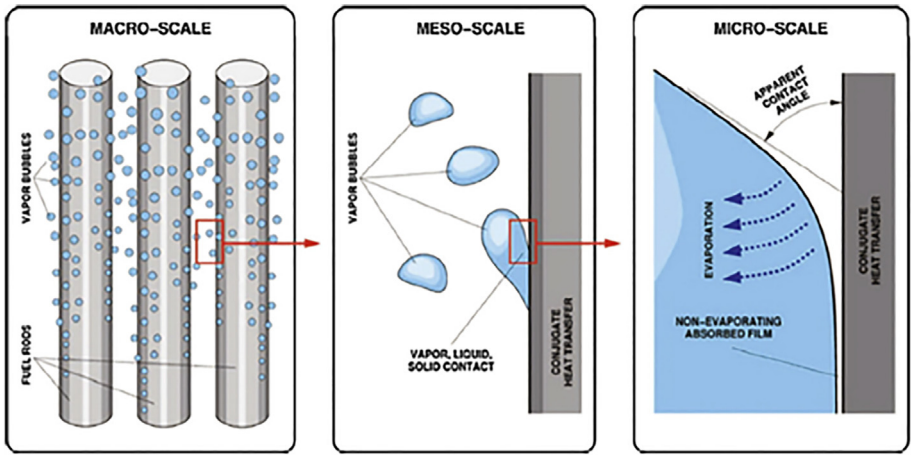

Fig. 1. Multi-scale modeling of rod bundle CHF [20].

Table 2
ATHAS modeling assumptions.

Thermal equilibrium model	Liquid/vapor thermal non-equilibrium
Single-phase friction factor	$f = 0.184Re^{-0.2}$
Two-phase friction factor multiplier	Homogeneous flow model
Two-phase form loss multiplier	Homogeneous flow model
Single-phase heat transfer correlation	Dittus-Boelter correlation
Two-phase heat transfer correlation	Chen correlation
Mixing model	Carlucci thermal/momentum and void drift mixing
Cross flow resistance factor	0.5

Table 3
Configuration of 5 × 5 CHF experiment.

No.	Element geometry	Axial flux shape	Heat length/ft	Intermediate mixing spacer grid
TEST 1	Typical	Uniform	12	NO
TEST 2	Typical	Uniform	14	NO
TEST 3	Typical	Uniform	12	YES
TEST 4	Guide tube	Uniform	12	NO
TEST 5	Typical	Cosine 1.55	12	NO

Table 4
Evaluation results of CHF test 1.

Method	M/P	Weisman & Pei	Lee & Mudawar	Lin et al.	Katto	KAIST
HBM	Mean	0.8712	0.7602	1.1191	0.7457	1.1347
	Standard deviation	0.0976	0.2049	0.0558	0.1952	0.0681
DSM	Mean	0.7628	0.7455	1.8165	0.7365	1.4021
	Standard deviation	0.2701	0.2199	0.3815	0.2025	0.1600

Lee & Mudawar and Katto model have little change compared with the HBM method, while those of Lin et al. and KAIST model have significant change. In general, the prediction results of Lin et al. and KAIST model are better than others when HBM method is used, and the standard deviation of M/P data predicted by KAIST model is smallest when DSM method is used.

It can also be seen from Table 4 that the M/P standard deviation of DSM method is significantly higher than that of HBM method, which can be intuitively understood through Fig. 2. When p, G, D and L are fixed, the change of q_c with x is investigated. Assuming that point A is the CHF experimental measured position, when x_i is determined, the heat flux corresponding to the intersection point A′ of the heat balance equation and the CHF prediction line is $q_{c,\mathrm{HBM}}$, while the heat flux corresponding to point A" of x_l is $q_{c,\mathrm{DSM}}$, obviously, $q_{c,\mathrm{HBM}}$ is closer to $q_{c,\mathrm{exp}}$. In the statistical analysis of M/P data,

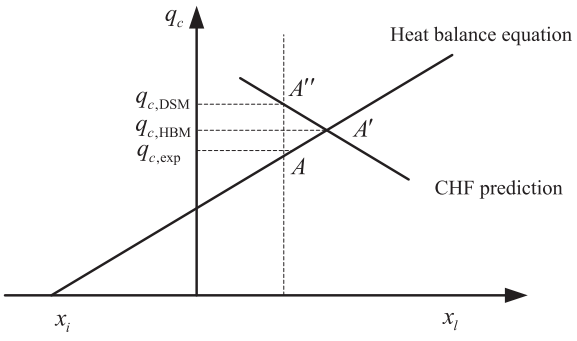

Fig. 2. Variation of x with q_c.

de Crécy [22] points out that the standard deviation calculated by the inlet condition is smaller than that corresponding to the local condition. Based on the inlet condition, the statistical performance of CHF prediction method is improved artificially, which is caused by heat balance equation rather than the ability of CHF correlation or mechanistic model itself.

In order to further assess the prediction performance of each CHF mechanistic model, the CHF experimental test 2 (typical geometry, uniform heating, heat length of 14 feet) and 3 (typical geometry, uniform heating, heat length of 12 feet, with intermediate mixing spacer grid) are evaluated with DSM method (if there is no special explanation, DSM method is used for subsequent calculation in this study). The evaluation results are shown in Table 5.

It can be seen that after the heat length is lengthened, the standard deviation of M/P data predicted by Weisman & Pei model is generally the largest and the average of M/P data of Lee & Mudawar and Katto model deviate from 1 seriously. With intermediate mixing spacer grid, the Lin et al. model can not accurately predict the CHF. Generally speaking, whether the heat length is lengthened or intermediate mixing spacer grid is added, the KAIST model performs better than other models.

4.2. Further verification of the KAIST model

To further verify the KAIST model, the CHF experimental test 4 (guide tube geometry, uniform heating, heat length of 12 feet) is evaluated. The results are shown in Fig. 3. It can be seen that the distribution of DNBR values calculated by the KAIST model are pretty good for the guide tube geometry, but the overall distribution of DNBR values are smaller than 1, obviously.

The evaluation results of CHF experimental test 5 (typical geometry, cosine 1.55 axial power distribution, heat length of 12 feet) are shown in Fig. 4. It can also be seen that the calculated DNBR values of the KAIST model are smaller than 1.

The comparison of CHF positions calculated by the KAIST model with the experimental measured positions of CHF test 5 are shown in Fig. 5.

It is not difficult to find that for the non-uniform axial power distribution, the CHF positions calculated by the KAIST model are in good agreement with the CHF experimental position without using non-uniform correction factor, and the deviation of most positions are only within one spacer grid span.

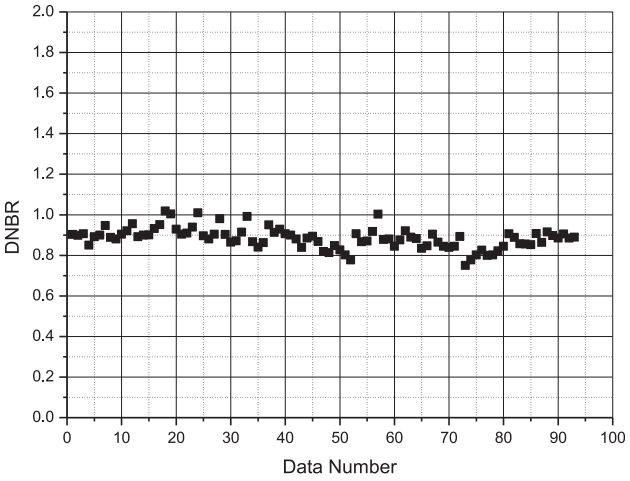

Fig. 3. Predicted DNBR value of CHF test 4.

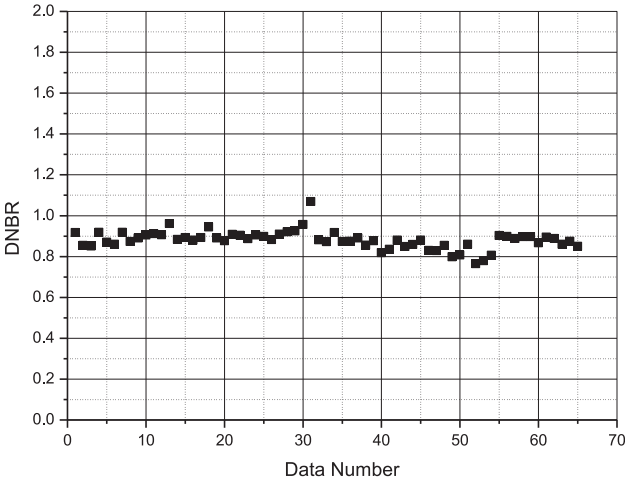

Fig. 4. Predicted DNBR value of CHF test 5.

5. Discussion

5.1. Comparative analysis

It can be seen from the basic assumptions and modeling process of each CHF mechanistic model that the bubble crowding model focuses on the state before the formation of vapor film, which corresponds to the heat flux before DNB, while the liquid sublayer dryout model focuses on the state after the formation of vapor film, which corresponds to the heat flux after DNB. As shown in Fig. 6, since CHF can be approximated from both ends of boiling heat transfer curve, both methods are feasible and representative.

To some extent, the superheated liquid layer depletion model is also a kind of liquid sublayer dryout model, because it assumes that there is no liquid contact heating surface when CHF occurs, which is similar to the liquid sublayer dryout model. However, it also considers the influence of upstream bubble generation and movement on CHF by integrating from OSV point to CHF point, which is similar to bubble crowding model. Therefore, it can be said that the superheated liquid layer depletion model is a CHF mechanistic model generated by the mechanism combination of the liquid sublayer dryout model and the bubble crowding model.

The commonness and difference analysis of the above three types CHF mechanistic models are shown in Table 6.

It can be seen from Table 6 that although the turbulence velocity fluctuations are considered in the bubble crowding model to transport the bulk flow to the bubble layer, the existence of liquid layer on the heating surface is ignored, and the influence of

Table 5
Evaluation results of CHF test 2 and 3.

CHF experimental data	M/P	Weisman & Pei	Lee & Mudawar	Lin et al.	Katto	KAIST
TEST 2	Mean	0.9203	0.5325	0.8877	0.5307	1.1139
	Standard deviation	0.5380	0.1294	0.2934	0.1630	0.0723
TEST 3	Mean	1.1171	0.9108	3.0391	0.9212	1.2837
	Standard deviation	0.3261	0.1721	0.9962	0.2153	0.1101

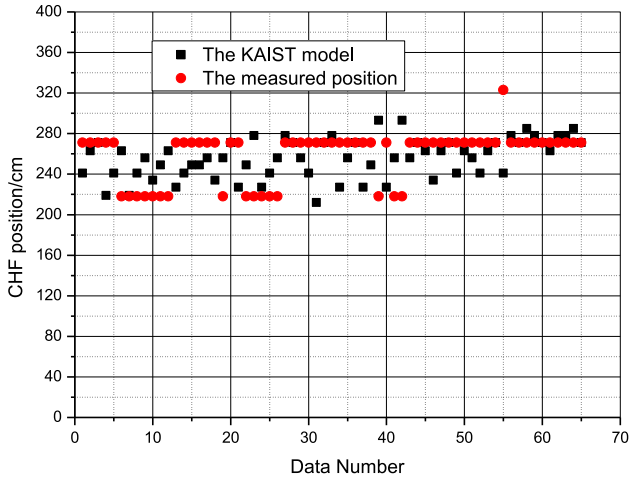

Fig. 5. CHF positions of CHF test 5.

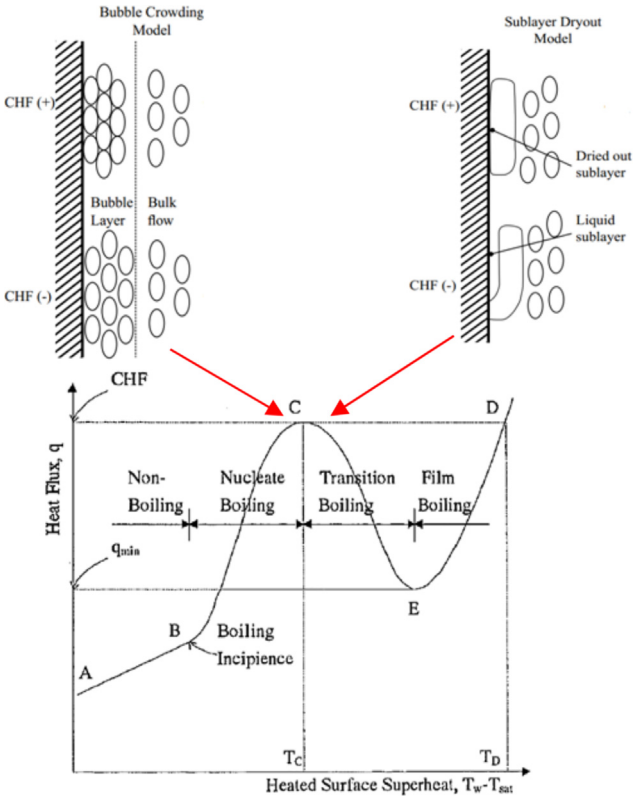

Fig. 6. Two ends of CHF approximate on boiling heat transfer curve.

upstream conditions on CHF is not fully considered. Although the liquid sublayer dryout model considers the existence of liquid layer on the heating surface, the supply of bulk flow to the heating surface and upstream conditions on CHF are ignored. Although the superheated liquid layer depletion model considers the influence of the liquid layer and upstream conditions on CHF, it ignores the turbulence velocity fluctuations to transport the bulk flow to the heating surface. All in all, the three types of CHF models have their own considerations, but at the same time, some key factors are ignored. This will provide enlightenment for the later development of CHF mechanistic model.

5.2. Improvement direction of the KAIST model

It can be seen from the comparative analysis in section 4 that the KAIST model can predict the CHF experimental data better than other CHF mechanistic models. However, the DNBR values predicted by the KAIST model are generally smaller than 1. As pointed out in section 5.1, the KAIST model ignores the turbulence velocity fluctuations to transport the bulk flow to the heating surface (as shown in Fig. 7), which reduces the mass flow rate of the superheated liquid layer, resulting in a smaller CHF prediction value.

The key of the KAIST model is to calculate the thickness and mass flow rate of the superheated liquid layer. However, when calculating the thickness of the superheated liquid layer at OSV point, the original KAIST model uses the Haramura & Katto correlation [23] initially developed for pool boiling, which will introduce some deviation.

To sum up, the KAIST model can be improved from two aspects: (1) considering the net mass exchange rate between the superheated liquid layer and the bulk flow; (2) developing the calculation correlation of the thickness of the superheated liquid layer applicable for rod bundle channel.

6. Conclusion

In this study, the five representative DNB type round tube CHF mechanistic models are selected to research rod bundle CHF mechanism. With properly conversion, the Weisman & Pei, Lee & Mudawar, Lin et al., Katto, and KAIST model are successfully coupled with subchannel analysis code ATHAS. The applicability of each CHF model is studied by using five tests of 5×5 full-length rod bundle CHF experimental data independently developed by NPIC and the commonness and difference of each CHF model are analyzed. Finally, the two improvement directions of the KAIST model are given.

The conclusions obtained are as follows:

(1) The round tube CHF mechanistic model based on the inlet condition can be converted into local condition to couple with the subchannel analysis code.
(2) Based on the assessment of typical/guide tube geometry, with/without intermediate mixing spacer grid, uniform/non-uniform heating and other CHF experimental conditions, the KAIST model has good CHF prediction performance and can well characterize the cold wall effect and non-uniform heating effect in the rod bundle channel without correction factors.
(3) The basic mechanism assumption of the KAIST model can provide reference for the development of rod bundle CHF mechanistic model, while the predicted DNBR values are generally smaller than 1.
(4) The KAIST model can be improved from two aspects: (a) considering the net mass exchange rate between the superheated liquid layer and the bulk flow; (b) developing the calculation correlation of the thickness of the superheated liquid layer applicable for rod bundle channel.

Declaration of competing interest

The authors declare that they have no known competing financial interests or personal relationships that could have appeared to influence the work reported in this paper.

Table 6
Comparison of different CHF mechanistic models.

Comparison term	liquid sublayer dryout model	bubble crowding model	superheated liquid layer depletion model
Region of interest (control volume)	Liquid sublayer between heating surface and intermittent vapor blanket	Bubble boundary layer	Superheated liquid layer near the wall
CHF triggering characteristic	During the passage time of the vapor blanket, the liquid sublayer complete evaporation	Bubbles in the bubble layer crowding to a critical value, which inhibit the supply of cooling water to the heating surface	The bubble layer inhibit the supply of the bulk flow to the heating surface, and the superheated liquid layer is depleted
The liquid layer on the heating surface	Liquid sublayer under vapor blanket	None	Superheated liquid layer
Supply of bulk flow to the heating surface	None	The turbulence fluctuations at the bubble layer-core interface transport the bulk flow to the bubble layer	None
Influence of upstream conditions on CHF	Assumption of local conditions (regardless of upstream condition)	Semi-local condition assumption (from bubble detachment point to critical bubble crowding point)	Integration of superheated liquid layer from OSV point to CHF point

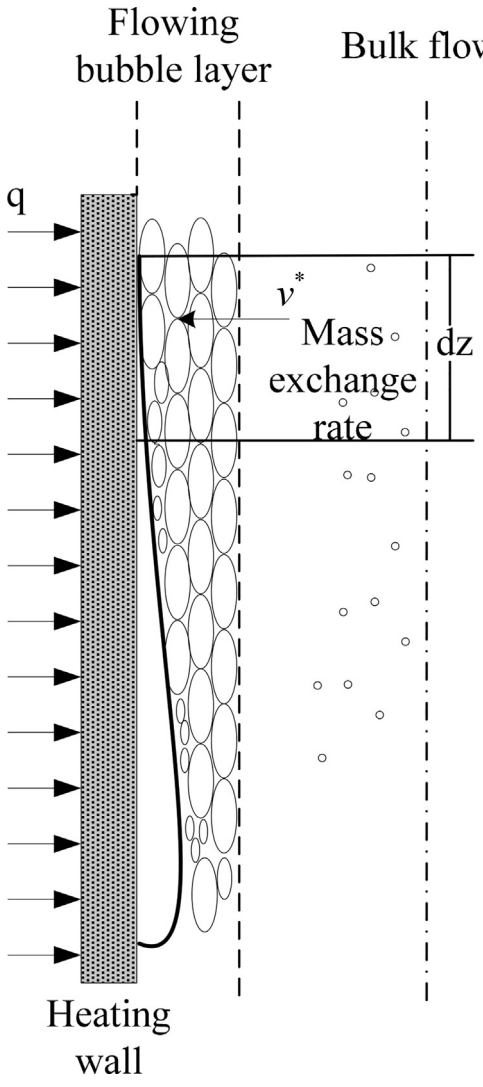

Fig. 7. Schematic diagram of interface net mass exchange rate.

Acknowledgments

The authors express their appreciation to Nuclear Power Institute of China for their financial support.

Appendix A. Supplementary data

Supplementary data to this article can be found online at https://doi.org/10.1016/j.net.2020.07.023.

References

[1] D. Groeneveld, The critical heat flux story, in: May 12-17: The 15th International Topical Meeting on Nuclear Reactor Thermal Hydraulics, 2013. Pisa, Italy.
[2] Wei Liu, Hideki Nariai, Ultrahigh CHF prediction for subcooled flow boiling based on homogenous nucleation mechanism, J. Heat Tran. 127 (2) (2005) 149–158.
[3] L.S. Tong, Heat transfer in water cooled nuclear reactors, Nucl. Eng. Des. 6 (4) (1967) 301–324.
[4] P.B. Whalley, The calculation of dryout in a rod bundle, Int. J. Multiphas. Flow 3 (6) (1977) 501–515.
[5] J. Saito, E.D. Hughes, M.W. Carbon, Multi-Fluid modeling of annular two-phase flow, Nucl. Eng. Des. 50 (2) (1978) 225–271.
[6] T. Mitsutake, H. Terasaka, K. Yoshimura, et al., Subchannel analysis of a critical power test using simulated BWR 8×8 fuel assembly, Nucl. Eng. Des. 122 (1–3) (1990) 235–254.
[7] H. Zhang, G. Hewitt, New models of droplet deposition and entrainment for prediction of CHF in cylindrical rod bundles, Nucl. Eng. Des. 305 (2016) 73–80.
[8] Wei Liu, Jianqiang Shan, Shinian Peng, et al., The study of critical heat flux in upflow boiling vertical round tube under high pressure, Sci. Technol. Nucl. Install. (2019) ID3695685.
[9] M. Bruder, G. Bloch, T. Sattelmayer, Critical heat flux in flow boiling-review of the current understanding and experimental approaches, Heat Tran. Eng. 38 (3) (2017) 347–360.
[10] T.H. Chun, W.P. Baek, S.H. Chang, An integral equation model for critical heat flux at subcooled and low quality flow boiling, Nucl. Eng. Des. 199 (1–2) (2000) 13–29.
[11] Jianqiang Shan, Bo Zhang, Changying Li, et al., SCWR subchannel code ATHAS development and CANDU-SCWR analysis, Nucl. Eng. Des. 239 (2009) 1979–1987.
[12] Wei Liu, B.A.I. Ning, Yuan-bing Zhu, et al., Research of reactor thermal-hydraulics sub-channel analysis code ATHAS, Nucl. Sci. Eng. 34 (1) (2014) 59–66.
[13] Jun Huang, Junli Gou, Wenjie Ding, et al., Development of a sub-channel analysis code based on the two-fluid model and its preliminary assessment, Nucl. Eng. Des. 340 (2018) 17–30.
[14] J. Weisman, B.S. Pei, Prediction of critical heat flux in flow boiling at low qualities, Int. J. Heat Mass Tran. 26 (10) (1983) 1463–1476.
[15] C.H. Lee, I. Mudawar, A mechanistic critical heat flux model for subcooled flow boiling based on local bulk conditions, Int. J. Multipliase Flow 14 (6) (1988) 711–728.
[16] W.S. Lin, C.H. Lee, B.S. Pei, An improved theoretical critical heat flux model for low quality flow, Nucl. Technol. 88 (1989) 294–306.
[17] Y. Katto, A prediction model of subcooled water flow boiling CHF for pressure in the range 0.1-20 MPa, Int. J. Heat Mass Tran. 35 (5) (1992) 1115–1123.
[18] D. Bestion, et al., Review of available data for validation of nuresim two-phase CFD software applied to CHF investigations, Sci. Technol. Nucl. Install. (2008), https://doi.org/10.1155/2009/214512.
[19] X. Cheng, U. Müller, Review on Critical Heat Flux in Water Cooled Reactors, FZKA, Karlsruhe, 2003.
[20] B. Niceno, Y. Sato, A. Badillo, et al., Multi-scale modeling and analysis of convective boiling: towards the prediction of CHF in rod bundles, Nucl. Eng.

Technol. 42 (6) (2010) 620–635.
[21] Wei Liu, Shinian Peng, Guangming Jiang, et al., Development and assessment of a new rod-bundle CHF correlation for China fuel assemblies, Ann. Nucl. Energy 138 (2020) ID107175.
[22] F. de Crécy, About critical heat flux correlations using inlet conditions, in: 31th Meeting of the European Two-phase Flow Group, 1994. Piacenza, Italy.
[23] Y. Haramura, Y. Katto, A new hydrodynamic model of critical heat flux, applicable widely to both pool and forced convention boiling on submerged bodies in saturated liquids, Int. J. Heat Mass Tran. 26 (1983) 389–399.

Nomenclature

ρ_v: Vapor density, kg/m^3
ρ_l: Liquid density, kg/m^3
p: Pressure, MPa
G: Mass flux, kg/m^{2}s
D: Tube diameter, mm
L: Heated length, m
α: Void fraction
x_i: Inlet thermodynamic quality
x_l: Local thermodynamic quality
M: Measured CHF, MW/m^2
P: Predicted CHF, MW/m^2
q: Heat flux, MW/m^2
q_c: Critical heat flux, MW/m^2